J. Applied Membrane Science & Technology, Vol. 25, No. 3, December 2021, 53–61

Surface Modification of Stainless-Steel Membrane using a Closed-Batch iCVD Reactor for Oil/Water Separation

M. Gürsoy[a,b], Ö. Saygı[a], R. Hoyladı[a], M. Yorulmaz[a] & M. Karaman[a,b*]

[a]Department of Chemical Engineering, Konya Technical University, 42030, Konya, Turkey
[b]Nanotechnology and Advanced Materials Development Application and Research Center, Konya Technical University, 42030, Konya, Turkey

Submitted: 25/6/2021. Revised edition: 26/7/2021. Accepted: 29/7/2021. Available online: 15/11/2021

ABSTRACT

Oil-spill is one of the major global issues facing society in this century. The aim of this study was to develop a steel-based membrane for selective separation of oil from oil/water mixture. For this purpose, a single-step, rapid and environmentally friendly closed-batch initiated chemical vapor deposition (iCVD) method was employed to deposit hydrophobic thin film on a stainless-steel mesh. Perfluorodecyl acrylate (PFDA) and tert-butyl peroxide (TBPO) were used as monomer and initiator, respectively. Owing to the inherent vapor-based nature of iCVD method provided excellent conformal coverage on the mesh with high durability. iCVD coated mesh showed 96% oil/water separation efficiency. Highly reproducible results were obtained when the oil/water separation experiments were repeated.

Keywords: Oil/water separation, iCVD, thin film, hydrophobic, mesh

1.0 INTRODUCTION

Industrial discharge of oily water and oil spillages adversely affect the environment and the health of all organisms. Oil-spill can have serious long-term negative impacts on the ecosystem due to the presence of various of hazardous and volatile organic compounds. Oil pollution can be accepted as one of the major global issues facing humanity in this century. International regulations have been prepared to prevent or minimize oil pollution [1]. In addition, in recent years, there has been growing interest in the oil-spill clean-up [2-4]. Various approaches have been proposed to collect or remove oil. The use of absorbent materials and membrane filtration are the most common ones. Fibres, zeolites, clays and human hair can be given as examples of absorbent materials [5-8]. However, use of absorbent materials in the oil-spill clean-up suffer from serious disadvantages. For instance, these materials can absorb not only oil but also water, which reduces their efficiency. Moreover, additional steps are necessary to regenerate these materials, which is undesirable property for continuous processes. On the other hand, membranes can be used for continuous oil/water separation and they have shown high oil-removal efficiency in the oil/water separation. For selective separation of oil from oil/water mixture, membranes are usually functionalized to change their wettabilities [9, 10]. The main aim of the functionalization is that the membranes repel one of the liquids while absorbing the other. These

* Corresponding to: M. Karaman (email: mkaraman@ktun.edu.tr)
DOI: https://doi.org/10.11113/amst.v25n3.224

membranes can be either hydrophobic/oleophilic or hydrophilic/oleophobic.

Various techniques have been proposed to functionalize membranes. These techniques can be categorized into two main groups: liquid-based processes and vapor-based processes. Initiated atom transfer radical polymerization (ATRP) [11], sol-gel [12], lithography [13], and dip-coating [14] can be given as examples of liquid-based processes. Although these methods can be easily applied and usually do not need any expensive and special equipment. Solvents used in these methods can fill the pores of substrate. However, the preservation of porous structure of membranes is very important. Moreover, hazardous and aggressive solvents may pose a threat to environment and human health. On the other hand, inherent solventless nature of vapor-based processes eliminates solution-related problems. As a vapor-based method, environmentally friendly and single-step chemical vapor deposition (CVD) is an efficient functionalization method. Moreover, CVD process can be easily scalable to achieve mass production using some equipment such as roll-to-roll process [15, 16]. So far, various types of CVD techniques have been applied to functionalize different types of membranes [17-22].

In this study, it was aimed that a commercial ordinary stainless-steel mesh was transformed into a hydrophobic/oleophilic thin film coated mesh for water/oil separation. Being inexpensive and abundant makes steel-based membrane a good choice for oil/water separation applications. Moreover, steel-based membranes have high mechanical strength and they can be durable in aggressive environmental conditions. Hence, they have been widely used in oil/water separation applications. For instance, Wang *et al*. deposited copper film on steel mesh, which showed high stability and durability under extreme environment conditions [23]. Gunatilake and Bandara coated steel mesh surface with TiO_2 nanofibers using spray coating method [24]. Tang *et al*. applied bacterially induced biomineralization method to modify steel mesh for oil/water separation [25]. Because of the aforementioned advantages of iCVD method, it was used to modify stainless steel meshes. Hydrophobic Poly (perfluorodecyl acrylate) (PPFDA) thin film was deposited on the mesh using single-step iCVD method. The oil/water separation performance of PPFDA coated mesh was tested. Hydrophobic/oleophilic PPFDA coated mesh developed by iCVD in this study showed a promising oil/water separation performance.

In typical iCVD reactor, the polymerization is conducted out by constantly feeding precursor into the vacuum chamber and simultaneously the reactor is continuously evacuated by a vacuum pump to remove unreacted chemicals and vapor-phase byproducts. During the polymerization, the flow rate of precursors is very important parameter affecting the final properties of the polymer. Thus, the calibration of the flow rate is necessary and they should be precisely adjusted. For this purpose, expensive valves and/or mass flow controllers are required in typical reactors. Furthermore, the flow rates should reach steady-state to produce reproducible polymeric thin films. In order to eliminate the problems related to reaching steady-state flow rate or calibration in typical iCVD reactor, an alternative approach namely, closed-batch iCVD reactor, was developed [20]. In closed-batch iCVD reactor, the reactor is filled by monomer and initiator in place of tuning precursor flow rates. According to literature on the iCVD deposition, as compared with

typical iCVD reactor, closed-batch iCVD reduced the costs associated with energy and chemical consumptions [26, 27]. Due to the advantages of closed-batch iCVD reactor, this strategy was applied in this study.

2.0 METHODS

2.1 Materials

A commercial stainless steel mesh membrane was used as substrate. Diesel was used as oil source and it was purchased from a local oil company. Monomer 1H,1H,2H,2H-perfluorodecyl acrylate (PFDA, 97%), and initiator di-tertbutyl peroxide (TBPO, 97%) were purchased from Sigma-Aldrich. The chemical structures of precursors are schematically given in Figure 1 (a) and (b).

2.2 Deposition of Hydrophobic Film

Polymeric thin film was deposited on stainless steel mesh surface using a custom-build iCVD system. The schematic diagram of iCVD system used in this study is given in Figure 1 (c). A more detailed description of the iCVD set-up has been described elsewhere [27]. A custom built cylindrical stainless-steel chamber having 50 cm outer diameter and 75 cm in height was used as the reactor.

Vacuum in the reactor was created by oil-sealed rotary vane vacuum pump (2XZ- 15C, EVP). The pressure in the reactor was measured by a capacitance type pressure gauge (MKS Baratron). The reactor has stainless-steel doors on both ends and the substrates were placed on a stage in the reactor by opening the reactor door. The backside of the stage has a heat exchanger, which was connected to a recirculating chiller (Lab. Companion RW-0525G, South Korea). The substrate temperature was set at 35 °C. The required energy for initiating for the polymerization was supplied from a heated nichrome filament array. The filament array was located 2.5 cm above the substrate. The filament temperature was kept constant at 200 °C using a PID temperature controller. The monomer and the initiator were vaporized in separate stainless-steel jars. The iCVD reactor was evacuated down to system base pressure, then the reactor was isolated from the pump. Monomer and initiator were fed into the reactor until the desired deposition pressure was reached. Monomer/initiator ratio was kept constant at 1/1 and the ratio was tuned based on monitoring the partial pressure of the precursors.

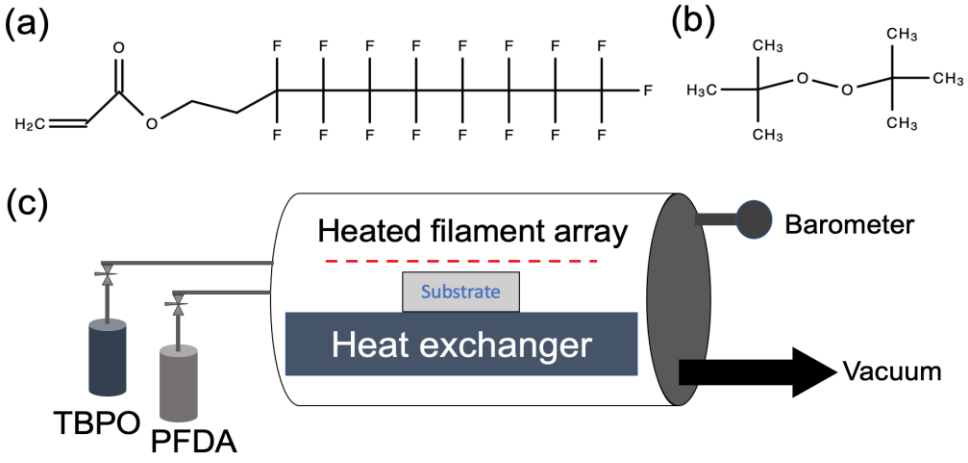

Figure 1 Chemical structures of PFDA (a) and TBPO (b). The schematic diagram of iCVD system (c)

2.3 Characterizations

Fourier transform infrared spectroscopy (FTIR) was used to reveal the chemical structures of as-deposited PPFDA thin film. FTIR measurements were conducted out using Bruker Vertex 70 with the help of a reflectance accessory in a range of 700 to 3700 cm^{-1}. Water contact angle measurements were performed by a contact angle goniometer device (Krüss Easy Drop) using 2.0 µl of pure water at ambient conditions.

10 mL oil/water mixture (with a volume ratio of 1/1) was poured over the inclined PPFDA coated mesh to perform oil/water separation efficiency experiment. Two separate containers were placed below the mesh to collect water and oil. When the experiments were completed, the volumes of the accumulated liquids in the containers were measured.

3.0 RESULTS AND DISCUSSION

3.1 PPFDA Coated Mesh

The photograph of stainless-steel mesh membrane used in this study is shown in Figure 2 (a). The opening size of the mesh is approximately 700 µm x 700 µm. After the mesh was coated with thin film using iCVD method, no change is observed in the general appearances of the mesh with naked eyes. The porous structure of the mesh is well-preserved, which indicates a conformal coating of thin film on the mesh. This observation is in agreement with the literature on the CVD deposition of porous materials [28, 29]. The water contact angle of PPFDA coated mesh was found to be 127.0° and the related image is given in Figure 2 (b).

Figure 3 shows the FTIR spectrum of PPFDA thin film. The FTIR spectrum was baseline. The spectra displayed the following major peak assignments: C-H stretching vibration (at around 2850-2950 cm^{-1}), C=O stretching (at around 1730 cm^{-1}, alkyl chains (at around 1458 and 1358 cm^{-1}), stretching vibrations -CF_2 (at around 1246 cm^{-1}), and -CF_2-CF_3 end group (at around 1161 cm^{-1}) [30-32]. The spectrum exhibits narrow, sharp and strong peaks, which belong to the functional groups of the chemical structure of PPFDA. Moreover, the spectrum does not contain C=C double bond, which implies that the polymerization proceeded through unsaturated C=C double bonds. Based on the FTIR spectrum, it can be said that a chemically well-defined polymeric thin film was produced using iCVD method.

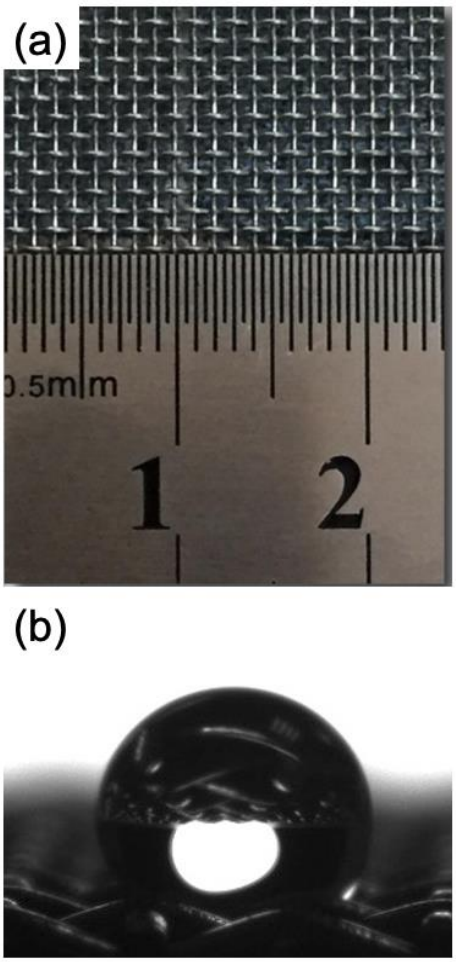

Figure 2 (a) Photograph of stainless-steel mesh and (b) the water contact angle of PPFDA coated mesh

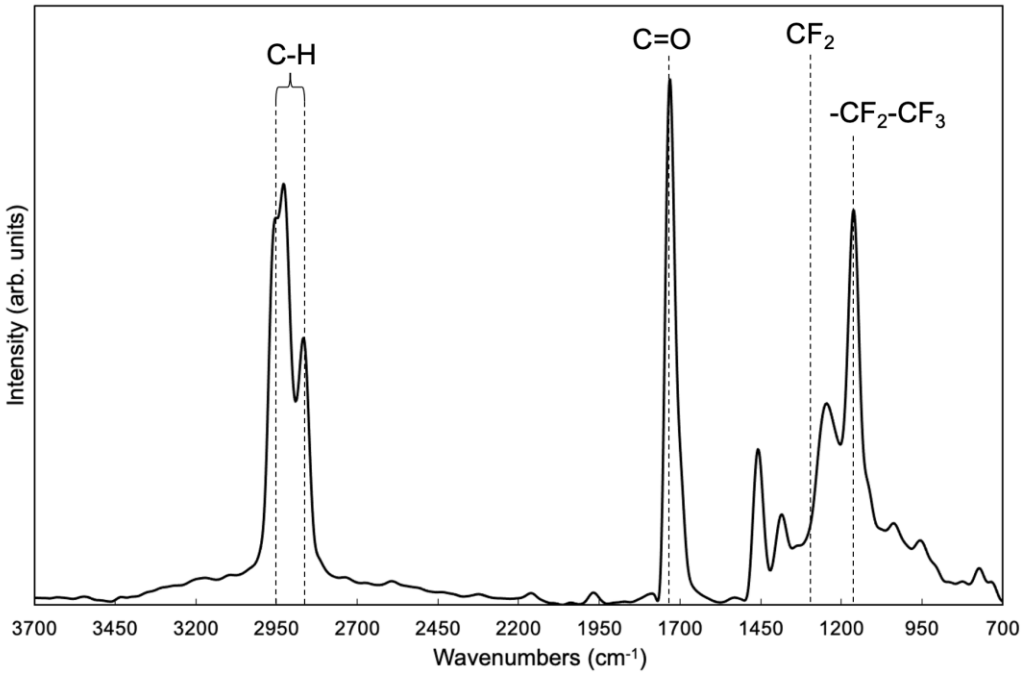

Figure 3 FTIR spectrum of PPFDA thin film

3.2 Oil/Water Separation Efficiency of PPFDA Coated Mesh

Figure 4 presents photographs of oil/water separation experiment. Oil/water mixture used in the experiment was shown in Figure 4 (a). In order to test oil/water separation efficiency, a mixture of oil and water was poured over PPFDA coated inclined mesh. During the oil/water separation process, while oil directly and rapidly passed through the mesh (Figure 4 (b)), the water stayed above the mesh due to the hydrophobic nature of the PPFDA coated mesh. The water droplets easily rolled off the mesh surface by inclination of the mesh (Figure 4 (c)). After the oil/water separation process, the amount of collected oil in the oil container was measured (Figure 4 (d)).

The oil/water separation efficiency (E) was defined as the ratio of the amount of collected oil in the oil container (O) to the initial amount of oil (O_0). The percentage of the oil/water separation efficiency was calculated according to Equation 1.

$$E(\%) = (O/O_0)x\,100 \quad (1)$$

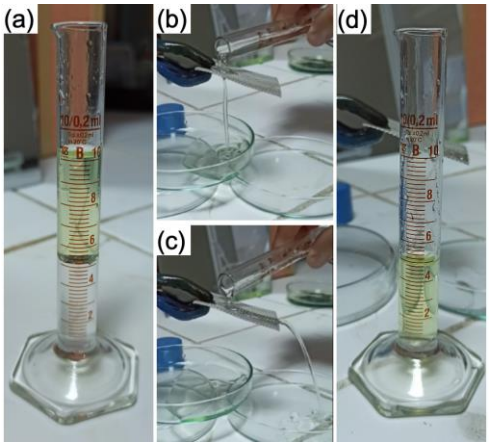

Figure 4 Photographs taken during oil/water separation process

The oil/water separation efficiency of PPFDA coated mesh was found as 96%. Only a small amount of the oil was dragged into the water-container along with the water flow. The durability of thin film on the mesh is a primary necessity for the reusability of the mesh. In order to test the reusability of mesh, the oil/water separation experiment was repeated 10 times for the same mesh. Very similar oil/water

separation efficiency values were found in each cycle. Highly reproducible results indicate that iCVD thin film was produced with high durability.

4.0 CONCLUSION

A single-step, rapid and environmentally friendly vapor-based closed-batch iCVD method was utilized to functionalize the mesh for oil/water separation purpose. According to the results of this study, it was shown that an ordinary stainless-steel mesh was successfully turned into a hydrophobic steel membrane which repels water while allowing the oil to penetrate through. The porosity of the mesh is well-preserved after the thin film deposition by iCVD. High (96%) and reproducible oil/water separation efficiency was obtained using PPFDA coated mesh. Oil/water separation was performed in a single step without the need of additional process, which indicates that the produced mesh in this study is highly incompatible with continuous-flow systems. Moreover, the developed technique in this study can be used to functionalize various kinds of meshes for different purposes.

ACKNOWLEDGEMENT

This work was supported in part by the Scientific and Technological Research Council of Turkey (TUBITAK) under the grant program 2209/A with project number 1919B011902296.

REFERENCES

[1] J. H. Hwang, K. Y. Kim, E. P. Resurreccion, W. H. Lee. 2019. Surfactant Addition to Enhance Bioavailability of Bilge Water in Single Chamber Microbial Fuel Cells (MFCs). *J. Hazard. Mater.* 368: 732-738. https://doi.org/10.1016/j.jhazmat.2019.02.007.

[2] T. D. Minh, M. C. Ncibi, V. Srivastava, B. Doshi, M. Sillanpää. 2021. Micro/nano-machines for Spilled-oil Cleanup and Recovery: A Review. *Chemosphere.* 129516. https://doi.org/10.1016/j.chemosphere.2020.129516.

[3] N. Zhang, Y. Qi, Y. Zhang, J. Luo, P. Cui, W. Jiang. 2020. A Review on Oil/Water Mixture Separation Material. *Ind. Eng. Chem. Res.* 59(33): 14546-14568. https://doi.org/10.1021/acs.iecr.0c02524.

[4] A. Dhaka, P. Chattopadhyay. 2021. A Review on Physical Remediation Techniques for Treatment of Marine Oil Spills. *J. Environ. Manage.* 288: 112428. https://doi.org/10.1016/j.jenvman.2021.112428.

[5] M. J. Nine, S. Kabiri, A. K. Sumona, T. T. Tung, M. M. Moussa, D. Losic. 2020. Superhydrophobic/superoleophilic Natural Fibres for Continuous Oil-water Separation and Interfacial Dye-adsorption. *Sep. Purif. Technol.* 233: 116062. https://doi.org/10.1016/j.seppur.2019.116062.

[6] S. Koushkbaghi, S. Jamshidifard, A. ZabihiSahebi, A. Abouchenari, M. Darabi, M. Irani. 2019. Synthesis of Ethyl cellulose/aluminosilicate Zeolite Nanofibrous Membranes for Oil–water Separation and Oil Absorption. *Cellulose.* 26(18): 9787-9801. https://doi.org/10.1007/s10570-019-02738-w.

[7] K. G. Akpomie, C. F. Onyeabor, C. C. Ezeofor, J. U. Ani, S. I. Eze. 2019. Natural Aluminosilicate

Clay Obtained from South-Eastern Nigeria as Potential Sorbent for Oil Spill Remediation. *J. African Earth Sci.* 155: 118-123. https://doi.org/10.1016/j.jafrearsci.2019.04.013.

[8] P. R. Ukotije-Ikwut, A. K. Idogun, C. T. Iriakuma, A. Aseminaso, T. Obomanu. 2016. A Novel Method for Adsorption using Human Hair as a Natural Oil Spill Sorbent. *Int J Sci Eng Res.* 7: 1754-1765. (https://www.ijser.org/researchpaper/A-Novel-Method-for-Adsorption-using-Human-Hair-as-a-Natural-Oil-Spill-Sorbent.pdf).

[9] Q. Ma, H. Cheng, A.G. Fane, R. Wang, H. Zhang. 2016. Recent Development of Advanced Materials with Special Wettability for Selective Oil/water Separation. *Small.* 12(16): 2186-2202. https://doi.org/10.1002/smll.201503685.

[10] S. N. W. Ikhsan, N. Yusof, F. Aziz, A. F. Ismail, J. Jaafar, W. N. W. Salleh, N. Misdan. 2021. Superwetting Materials for Hydrophilic-Oleophobic Membrane in Oily Wastewater Treatment. *J. Environ. Manage.* 290:112565. https://doi.org/10.1016/j.jenvman.2021.112565.

[11] Z. Yang, D. Saeki, H.-C. Wu, T. Yoshioka, H. Matsuyama. 2019. Effect of Polymer Structure Modified on RO Membrane Surfaces via Surface-initiated ATRP on Dynamic Biofouling Behavior. *J. Membr. Sci.* 582: 111-119. https://doi.org/10.1016/j.memsci.2019.03.094.

[12] A. Xie, J. Cui, Y. Chen, J. Lang, C. Li, Y. Yan, J. Dai. 2019. One-Step Facile Fabrication of Sustainable Cellulose Membrane with Superhydrophobicity via a Sol-gel Strategy for Efficient Oil/Water Separation. *Surf. Coat. Tech.* 361: 19-26.https://doi.org/10.1016/j.surfcoat.2019.01.040.

[13] J. Hutfles, W. Chapman, J. Pellegrino. 2018. Roll-to-roll Nanoimprint Lithography of Ultrafiltration Membrane. *J. Appl. Polym. Sci.* 135(11): 45993. https://doi.org/10.1002/app.45993.

[14] I. Wenten, K. Khoiruddin, A. Wardani, P. Aryanti, D. Astuti, A. Komaladewi. 2020. Preparation of Antifouling Polypropylene/ZnO Composite Hollow Fiber Membrane by Dip-Coating Method For Peat Water Treatment. *J. Water Process. Eng.* 34: 101158. https://doi.org/10.1016/j.jwpe.2020.101158.

[15] H. Şakalak, K. Yılmaz, M. Gürsoy, M. Karaman. 2020. Roll-to roll Initiated Chemical Vapor Deposition of Super Hydrophobic Thin Films on Large-Scale Flexible Substrates. *Chem. Eng. Sci.* 215: 115466. https://doi.org/10.1016/j.ces.2019.115466.

[16] S. K. Cho, T. Y. Cho, W. J. Lee, M. S. Um, W. J. Choi, J. H. Lee, J. Ryu, S. H. Choa. 2019. Gas Barrier and Mechanical Properties of a Single‐Layer Silicon Oxide Film Prepared by Roll-to-roll PECVD System. *Plasma Process Polym.* 16(4): 1800170. https://doi.org/10.1002/ppap.201800170.

[17] N. Said, Y. S. Khoo, W. J. Lau, M. Gürsoy, M. Karaman, T. M. Ting, E. Abouzari-Lotf, A. F. Ismail. 2020. Rapid Surface

Modification of Ultrafiltration Membranes for Enhanced Antifouling Properties. *Membranes.* 10(12): 401. https://doi.org/10.3390/membranes10120401.

[18] W. Liu, C. Su, P. Su, H. Yang, P. Lu, Z. Du, Y. Ye. 2021. Sub-20 nm Bilayer Hydrophilic Poly (Vinyl Pyrrolidone) Coatings for Antifouling Nanofiltration Membranes. *Macromol Mater Eng.* 2100026. https://doi.org/10.1002/mame.202100026.

[19] Y. S. Khoo, W. J. Lau, Y. Y. Liang, M. Karaman, M. Gürsoy, A. F. Ismail. 2020. A Green Approach to Modify Surface Properties of Polyamide Thin Film Composite Membrane for Improved Antifouling Resistance. *Sep. Purif. Technol.* 250: 116976. https://doi.org/10.1016/j.seppur.2020.116976.

[20] Y. S. Khoo, M. Q. Seah, W. J. Lau, Y. Y. Liang, M. Karaman, M. Gürsoy, J. Meng, H. Gao, A. F. Ismail. 2021. Environmentally Friendly Approach for the Fabrication of Polyamide Thin Film Nanocomposite Membrane with Enhanced Antifouling and Antibacterial Properties. *Sep. Purif. Technol.* 260: 118249. https://doi.org/10.1016/j.seppur.2020.118249.

[21] Y. S. Khoo, W. J. Lau, Y. Y. Liang, M. Karaman, M. Gürsoy, G. S. Lai, A. F. Ismail. 2021. Rapid and Eco-friendly Technique for Surface Modification of TFC RO Membrane for Improved Filtration Performance. *J. Environ. Chem. Eng.* 9(3): 105227. https://doi.org/10.1016/j.jece.2021.105227.

[22] A. T. Servi, E. Guillen-Burrieza, D. M. Warsinger, W. Livernois, K. Notarangelo, J. Kharraz, H. A. Arafat, K. K. Gleason. 2017. The Effects of iCVD Film Thickness and Conformality on the Permeability and Wetting of MD Membranes. *J. Membr. Sci*. 523: 470-479. https://doi.org/10.1016/j.memsci.2016.10.008.

[23] J. Wang, Z. Zou, G. Geng. 2019. Construction of Superhydrophobic Copper Film on Stainless Steel Mesh by a Simple Liquid Phase Chemical Reduction for Efficient Oil/Water Separation. *Appl. Surf. Sci*. 486: 394-404. https://doi.org/10.1016/j.apsusc.2019.05.045.

[24] U. B. Gunatilake, J. Bandara. 2017. Efficient Removal of Oil from Oil Contaminated Water by Superhydrophilic and Underwater Superoleophobic Nano/Micro Structured TiO2 Nanofibers Coated Mesh. *Chemosphere.* 171: 134-141. https://doi.org/10.1016/j.chemosphere.2016.12.031.

[25] S. Tang, X. Chang, M. Li, T. Ge, S. Niu, D. Wang, Y. Jiang, S. Sun. 2021. Fabrication of Calcium Carbonate Coated-stainless Steel Mesh for Efficient Oil-water Separation via Bacterially İnduced Biomineralization Technique. *Chem. Eng. J.* 405: 126597. https://doi.org/10.1016/j.cej.2020.126597

[26] C. D. Petruczok, N. Chen, K. K. Gleason. 2014. Closed Batch Initiated Chemical Vapor Deposition of Ultrathin, Functional, and Conformal Polymer Films. *Langmuir*. 30(16): 4830-4837.

https://doi.org/10.1021/la500543d.

[27] K. Yılmaz, H. Şakalak, M. Gürsoy, M. Karaman. 2019. Initiated Chemical Vapor Deposition of Poly (Ethylhexyl Acrylate) Films in a Large-scale Batch Reactor. *Ind. Eng. Chem. Res.* 58(32): 14795-14801. https://doi.org/10.1021/acs.iecr.9b02213.

[28] Z. C. Ng, R. A. Roslan, W. J. Lau, M. Gürsoy, M. Karaman, N. Jullok, A.F. Ismail. 2020. A Green Approach to Modify Surface Properties of Polyurethane Foam for Enhanced Oil Absorption. *Polymers.* 12(9): 1883. https://doi.org/10.3390/polym12091883.

[29] P. Moni, A. Al-Obeidi, K.K. Gleason. 2017. Vapor Deposition Routes to Conformal Polymer Thin Films. *Beilstein J. Nanotechnol.* 8(1): 723-735. https://doi.org/10.3762/bjnano.8.76.

[30] M. Gupta, K. K. Gleason. 2006. Initiated Chemical Vapor Deposition of Poly(1H,1H,2H,2H-perfluorodecyl Acrylate) Thin Films. *Langmuir.* 22(24): 10047-10052. https://doi.org/10.1021/la061904m.

[31] H. Sojoudi, S. Kim, H. Zhao, R. K. Annavarapu, D. Mariappan, A. J. Hart, G. H. McKinley, K. K. Gleason. 2017. Stable Wettability Control of Nanoporous Microstructures by iCVD Coating of Carbon Nanotubes. *ACS Appl. Mater. Interfaces*. 9(49): 43287-43299. https://doi.org/10.1021/acsami.7b13713.

[32] E. Çıtak, B. İstanbullu, H. Şakalak, M. Gürsoy, M. Karaman. 2019. All-dry Hydrophobic Functionalization of Paper Surfaces for Efficient Transfer of CVD Graphene. Macromolecular Macromol. *Chem. Phys.* 220(22): 1900277. https://doi.org/10.1002/macp.201900277.